NACA

RESEARCH MEMORANDUM

SOME EFFECTS OF SPANWISE AILERON LOCATION AND

WING STRUCTURAL RIGIDITY ON THE ROLLING EFFECTIVENESS

OF 0.3-CHORD FLAP-TYPE AILERONS ON A TAPERED WING

HAVING 63° SWEEPBACK AT THE LEADING EDGE AND

NACA 64A005 AIRFOIL SECTIONS

By H. Kurt Strass, E. M. Fields, and Eugene D. Schult

Langley Aeronautical Laboratory
Langley Field, Va.

NATIONAL ADVISORY COMMITTEE
FOR AERONAUTICS
WASHINGTON

NATIONAL ADVISORY COMMITTEE FOR AERONAUTICS

RESEARCH MEMORANDUM

SOME EFFECTS OF SPANWISE AILERON LOCATION AND

WING STRUCTURAL RIGIDITY ON THE ROLLING EFFECTIVENESS

OF 0.3-CHORD FLAP-TYPE AILERONS ON A TAPERED WING

HAVING 63° SWEEPBACK AT THE LEADING EDGE AND

NACA 64A005 AIRFOIL SECTIONS

By H. Kurt Strass, E. M. Fields, and Eugene D. Schult

SUMMARY

Some effects of aileron spanwise location and wing structural rigidity on the rolling power of 0.3-chord plain, flap-type ailerons on a wing with a taper ratio of 0.25, an aspect ratio of 3.5, and swept back 63° at the leading edge have been investigated by the Langley Pilotless Aircraft Research Division by the use of rocket-propelled test vehicles.

The results show that, for rigid wings, aileron spanwise location is a significant consideration with the maximum rolling effectiveness per unit aileron span occurring at approximately mid-exposed span. At speeds above Mach number of approximately 0.9 the 0.314-semispan inboard aileron was more effective than the 0.50-semispan outboard aileron. The relative effectiveness of the inboard aileron increased with Mach number until, at Mach number of 1.6, the inboard aileron was approximately 150 percent more effective than the outboard aileron. The large effect of wing flexibility on control effectiveness is demonstrated by the fact that for solid aluminum-alloy wings the loss of control effectiveness of an outboard 0.50-semispan aileron exceeds 30 percent of the rigid-wing values at a Mach number of 1.4.

INTRODUCTION

Much research effort has been expended at the Ames Aeronautical Laboratory evaluating the performance of a thin, highly tapered, highly

swept wing and several versions of this wing have been investigated
(see, for example, references 1 and 2). In an extension of this work,
the Langley Pilotless Aircraft Research Division has investigated the
rolling effectiveness of a wing similar to that of reference 2 and
equipped with 0.3-chord, plain, flap-type ailerons in the speed range
between $0.8 \lesssim M \lesssim 1.6$ by means of rocket-propelled test vehicles. The
wings tested were swept back 63° at the leading edge, had a taper ratio
of 0.25, employed the NACA 64A005 airfoil section parallel to the model
center line, and had several values of stiffness.

SYMBOLS

A   aspect ratio, $\left(\dfrac{b^2}{S} = 3.5\right)$

b   diameter of circle swept by wing tips, 2.25 feet

i_w average wing incidence for three wings measured in plane of
δ_a, positive when tending to produce clockwise roll as seen
from the rear, degrees

M   Mach number

m   concentrated couple, applied near wing tip in a plane parallel
to the body center line and normal to wing-chord plane,
foot-pounds

P   static pressure, pounds per square foot

p   rolling velocity, radians per second

pb/2V   wing tip helix angle, radians

S   area of two wing panels measured to fuselage center line,
1.44 square feet

V   flight-path velocity, feet per second

y   spanwise position of end of aileron measured normal to model
center line, feet

$\dfrac{dc_m/d\delta}{d\alpha/d\delta}$ section twisting-moment parameter for constant lift

$dc_m/d\delta$ rate of change of section pitching-moment coefficient with
            aileron angle, per radian

$d\alpha/d\delta$ rate of change of wing angle of attack with aileron angle as
            obtained for constant lift at section

δ_a deflection of each aileron measured in a plane perpendicular
            to the chord plane and parallel to the model center line
            (average for three wings), degrees

φ fraction of rigid-wing rolling effectiveness retained by
            flexible wing

Λ sweep of wing leading edge, degrees

λ ratio of tip chord to root chord at model center line

θ angle of twist, produced by m, at any section along wing span
            in a plane parallel to free stream and normal to wing-chord
            plane, radians

$1/m_\theta$ wing-torsional-stiffness parameter, measured parallel to model
            center line, radians per foot-pound (θ/m)

Subscripts:

a   altitude $\left(\text{except } \delta_a\right)$

0   sea level

r   reference station (exposed aileron midspan)

i   inboard

MODELS AND TECHNIQUE

The test vehicles used in the present investigation are shown in
the photograph presented as figure 1 and in the sketch of figure 2.
The total exposed wing area for three panels was 1.56 square feet, the
area of two wings taken to the center line of the fuselage was 1.44
square feet, and the aspect ratio was 3.5. The ailerons had 0.3 free-
stream chord and simulated sealed faired ailerons in that there was no
surface discontinuity at the aileron hinge axis. The airfoil section
parallel to the model center line for all models was the NACA 64A005.

Depending upon the value of wing torsional rigidity desired, the material of which the test wings were constructed was either solid steel, solid aluminum alloy, or composite construction of aluminum alloy and beech. The latter type of contruction is illustrated in figure 3 in conjunction with a general description of the test wings.

The torsional-stiffness parameters of all the test wings were obtained by applying a known couple at the wing tip and by measuring the resulting twist along the span. The couple was applied and the twist was measured in a plane parallel to the free stream and normal to the wing-chord plane. The variation of the torsional-stiffness parameter $1/m_\theta$ with exposed span measured normal to the model center line is presented in figure 4 for the three methods of construction employed.

The flight tests were made at the Pilotless Aircraft Research Station at Wallops Island, Va. The test vehicles were propelled by a two-stage rocket-propulsion system to a Mach number of about 1.7. During a 10-second period of coasting flight following rocket-motor burnout, time histories of the rolling velocity were obtained with special radio equipment and the flight-path velocity was obtained by the use of CW Doppler radar. These data, in conjunction with atmospheric data obtained with radiosondes, permitted the evaluation of the aileron rolling effectiveness in terms of the parameter $pb/2V$ as a function of Mach number. The Reynolds number for the tests varied from approximately 3×10^6 at $M = 0.7$ to 6.6×10^6 at $M = 1.6$. Reference 3 gives a more complete description of the flight testing technique.

ACCURACY AND CORRECTIONS

Based upon previous experience, the maximum experimental error is estimated to be within the following limits:

	Subsonic	Supersonic
$pb/2V$	±0.0050	±0.0025
M	±.005	±.005

The sensitivity of the experimental technique, however, is such that much smaller irregularities in the variation of $pb/2V$ with Mach number may be detected. For purposes of economy and ease of construction, small variations from the desired values of $0°$ and $5°$ for wing

incidence and control deflection, respectively, were permitted. The data were corrected for effect of wing incidence i_w by use of the following equation which was derived from strip theory for rigid wings:

$$\Delta \frac{pb}{2V} = \frac{2}{57.3} i_w \frac{1 + 2\lambda}{1 + 3\lambda} = 0.0299 i_w \text{ radians}$$

The validity of this correction has been verified in reference 4. The corrections for aileron deflection were made by reducing the data to $\frac{pb/2V}{\delta_a}$ and then multiplying by the nominal δ_a value of $5°$. All the data presented have been corrected to nominal incidence and aileron-setting values of $0°$ and $5°$, respectively. The actual measured values for the models tested are presented in table I.

No attempt was made to correct for the effect of test-vehicle moment of inertia about the roll axis on the measured variation of pb/2V with Mach number since the method of analysis suggested in reference 3 indicated that the magnitude of the correction is negligible.

The pb/2V values of figures 5 through 8 have not been corrected to sea-level conditions.

RESULTS AND DISCUSSION

Aeroelastic Effects

The variation of pb/2V with Mach number and the effect of wing stiffness on pb/2V are shown in figures 5 through 8, along with the pressure ratio P_a/P_0 at which corresponding pb/2V values were obtained, for the various configurations tested. From the data in these figures it can be seen that a wing of the present type will encounter large rolling-effectiveness losses unless the construction is extremely rigid. For example, at sea level, the loss in control effectiveness due to wing flexibility exceeds 30 percent of the rigid-wing value at $M = 1.4$ for the outboard $0.50\frac{b}{2}$ aileron when used with a wing constructed of solid aluminum alloy.

The rigid-wing values, obtained by the method of reference 4 for the $0.50\frac{b}{2}$ outboard aileron, are used to obtain the relative loss in control effectiveness $(1 - \varphi)$ due to wing twisting and these $(1 - \varphi)$ values are in turn substituted in equation (1) of reference 5 to give $\frac{dc_m/d\delta}{d\alpha/d\delta}$. These $\frac{dc_m/d\delta}{d\alpha/d\delta}$ values are then used in conjunction with the

information presented in reference 5 to estimate the rigid-wing values
for the other aileron configurations tested. It was necessary to extend
the calculations of reference 5 to include the case of the $0.314\frac{b}{2}$
inboard aileron.

The values of $\dfrac{dc_m/d\delta}{d\alpha/d\delta}$ obtained from this investigation are com-
pared in figure 9 with similar data from reference 4. These data indi-
cate that the twisting moment produced by the aileron decreases as the
wing sweepback increases. Because of the method of derivation, the
values are only strictly applicable to wings of the same sweep, aspect
ratio and stiffness variation as the test wings; however, it is believed
that minor variations in these parameters should not affect the value of
these data. For design purposes, the values of figure 9 should be used
in conjunction with equation 1 of reference 5 when estimating the loss
of wing-aileron rolling effectiveness due to wing flexibility.

Aileron Span and Spanwise Location

Figure 10 summarizes the rigid-wing rolling-effectiveness results
for the various wing-aileron configurations. Values in reference 2,
presented for comparison, were obtained by measuring the rolling moment
on a constrained model and by using calculated damping coefficients to
calculate the pb/2V. In addition, results obtained at M = 0.3 in
the Langley 7- by 10-foot tunnel for the same models are presented as
an aid in estimating the rolling effectiveness in the region for which
no data are available $(0.3 \leq M \leq 0.9)$. The low-speed wind-tunnel
rolling-effectiveness data were obtained by mounting the rocket models
upon a sting which allowed the models to revolve freely with negligible
friction. The agreement between the two testing techniques has been
found to be good in previous tests where data at the same Mach number
were available. References 6 and 7 give a more complete description of
the low-speed wind-tunnel testing technique and the agreement between
the free-flight and wind-tunnel data. The agreement between the super-
sonic wind-tunnel data of reference 2 and comparable free-flight data
is good. At M = 0.3, the wind-tunnel tests show the outboard aileron
to be approximately 60 percent more effective than the inboard aileron,
but at M = 0.95 the flight tests show that the two aileron configu-
rations had equal effectiveness. Above M = 0.95, the inboard aileron
became relatively more effective with increasing Mach number until, at
the highest Mach number tested (M = 1.6), the inboard aileron was
approximately 150 percent more effective than the outboard. A similar
condition was encountered previously in the free-flight tests of a 45°
sweptback untapered wing, for which data are presented in reference 8.

The results for the two lengths of outboard ailerons and the
$0.814\frac{b}{2}$ aileron from figure 10 are replotted in figure 11 as the

variation of pb/2V with the corresponding spanwise location of the
inboard end of the aileron. The rolling effectiveness of a given aileron
or segment of aileron is determined by the increment in pb/2V between
the inboard and outboard ends. The region of maximum aileron effective-
ness per unit span occurs where the slope of the curve has the highest
value and, for this configuration, is approximately at midspan. It
should be noted that the outer part of the ailerons become proportion-
ally less effective with increasing Mach number until, at the highest
Mach number for which data are available, this part is almost inef-
fective as a roll-producing device. Figure 12 presents the measured
variation of pb/2V with Mach number for the inboard $0.314\frac{b}{2}$ aileron
as compared with the estimated variation obtained from figure 11, where
the estimated value is equal to the difference between the values of
pb/2V corresponding to the inboard and outboard ends of the inboard
$0.314\frac{b}{2}$ aileron. Satisfactory agreement is obtained between the esti-
mated and measured values.

CONCLUSIONS

An investigation of some effects of spanwise aileron location and
structural rigidity on the control effectiveness of 0.3-chord, plain,
faired, flap-type ailerons on a wing swept back 63° at the leading edge
with a taper ratio of 0.25 and having an aspect ratio of 3.5 gave the
following conclusions:

1. The spanwise location of the ailerons was critical, with the
maximum rolling effectiveness per unit span occurring at approximately
mid-exposed span in the Mach number range tested.

2. At speeds above Mach number of approximately 0.95, the 0.314-
semispan inboard ailerons were more effective than the 0.50-semispan
outboard ailerons with the relative effectiveness of the inboard aileron
increasing until, at the highest speed for which data are available
(M = 1.6), the inboard aileron was approximately 150 percent more effec-
tive than the outboard.

3. The measured variation of rolling effectiveness with Mach number
for the 0.314-semispan inboard ailerons agreed satisfactorily with that
estimated from generalized effectiveness curves obtained from tests of
outboard and full-span ailerons.

4. The control-effectiveness of the particular wing-control con-
figurations for which data are presented are greatly influenced by wing
flexibility. For example, the 0.50-semispan outboard aileron experienced

a loss in rolling effectiveness of more than 30 percent at $M \approx 1.4$
when used with a wing constructed of solid aluminum alloy.

National Advisory Committee for Aeronautics
     Langley Aeronautical Laboratory
          Langley Field, Va.

REFERENCES

1. Jones, J. Lloyd, and Demele, Fred A.: Aerodynamic Study of a Wing-
   Fuselage Combination Employing a Wing Swept Back 63°. - Character-
   istics throughout the Subsonic Speed Range with the Wing Cambered
   and Twisted for a Uniform Load at a Lift Coefficient of 0.25.
   NACA RM A9D25, 1949.

2. Olson, Robert N., and Mead, Merrill H.: Aerodynamic Study of a Wing-
   Fuselage Combination Employing a Wing Swept Back 63°. - Effectiveness
   at Supersonic Speeds of a 30 Percent Chord, 50-Percent Semispan
   Elevon as a Lateral Control Device. NACA RM A50K07, 1951.

3. Sandahl, Carl A., and Marino, Alfred A.: Free-Flight Investigation
   of Control Effectiveness of Full-Span 0.2-Chord Plain Ailerons at
   High Subsonic, Transonic, and Supersonic Speeds to Determine Some
   Effects of Section Thickness and Wing Sweepback. NACA RM L7D02,
   1947.

4. Strass, H. Kurt, Fields, E. M., and Purser, Paul E.: Experimental
   Determination of Effect of Structural Rigidity on Rolling Effective-
   ness of Some Straight and Swept Wings at Mach Numbers from 0.7
   to 1.7. NACA RM L50G14b, 1950.

5. Pearson, Henry A., and Aiken, William S., Jr.: Charts for the
   Determination of Wing Torsional Stiffness Required for Specified
   Rolling Characteristics or Aileron Reversal Speed. NACA Rep. 799,
   1944.

6. Johnson, Harold S.: Wind-Tunnel Investigation at Low Transonic
   Speeds of the Effects of Number of Wings on the Lateral-Control
   Effectiveness of an RM-5 Test Vehicle. NACA RM L9H16, 1949.

7. Johnson, Harold S.: Wind-Tunnel Investigation at Subsonic and Low
   Transonic Speeds of the Effects of Aileron Span and Spanwise
   Location on the Rolling Characteristics of a Test Vehicle with
   Three Untapered 45° Sweptback Wings. NACA RM L51B16, 1951.

8. Strass, H. Kurt: The Effect of Spanwise Aileron Location on the
   Rolling Effectiveness of Wings with 0° and 45° Sweep at Subsonic,
   Transonic, and Supersonic Speeds. NACA RM L50A27, 1950.

TABLE I

DESCRIPTION OF INDIVIDUAL TEST VEHICLES

Aileron configuration	$1/m_{\theta_r}$	i_w (deg)	δ_a (deg)	Type of construction
Inboard $0.314\frac{b}{2}$	2.3×10^{-4}	0.07	4.93	Solid aluminum alloy
Outboard $0.50\frac{b}{2}$	7.2 25.5 (model 1) 25.5 (model 2) 128.0	-.14 -.13 .19 -.02	4.80 4.39 4.45 4.66	Solid steel Solid aluminum alloy Solid aluminum alloy Beech, aluminum-alloy core
Outboard $0.25\frac{b}{2}$	50.0	.06	6.17	Solid aluminum alloy
$0.814\frac{b}{2}$ (Full exposed span)	9.0	.12	5.22	Solid aluminum alloy
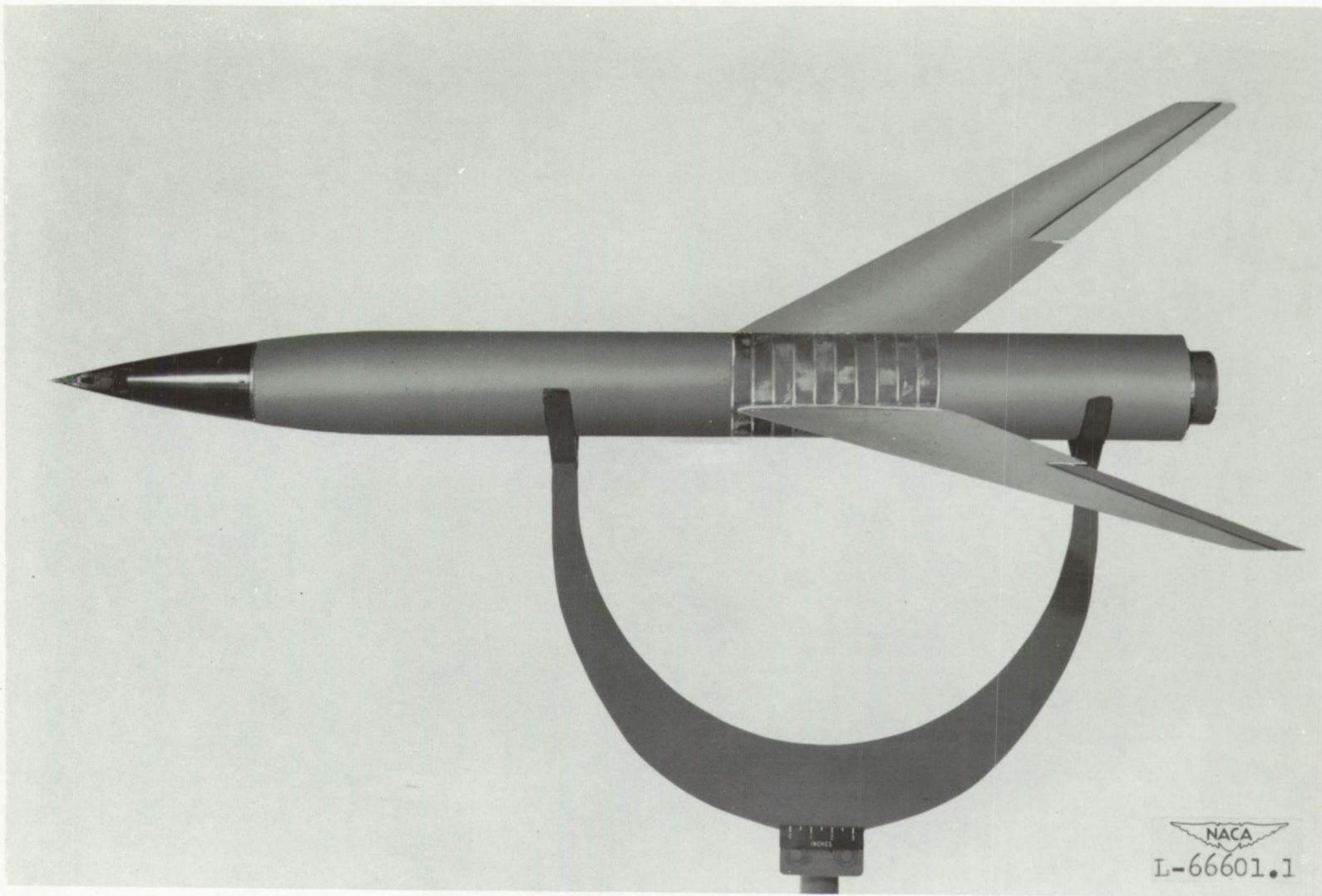
Figure 1.- Photograph of typical test vehicle.

Page intentionally left blank
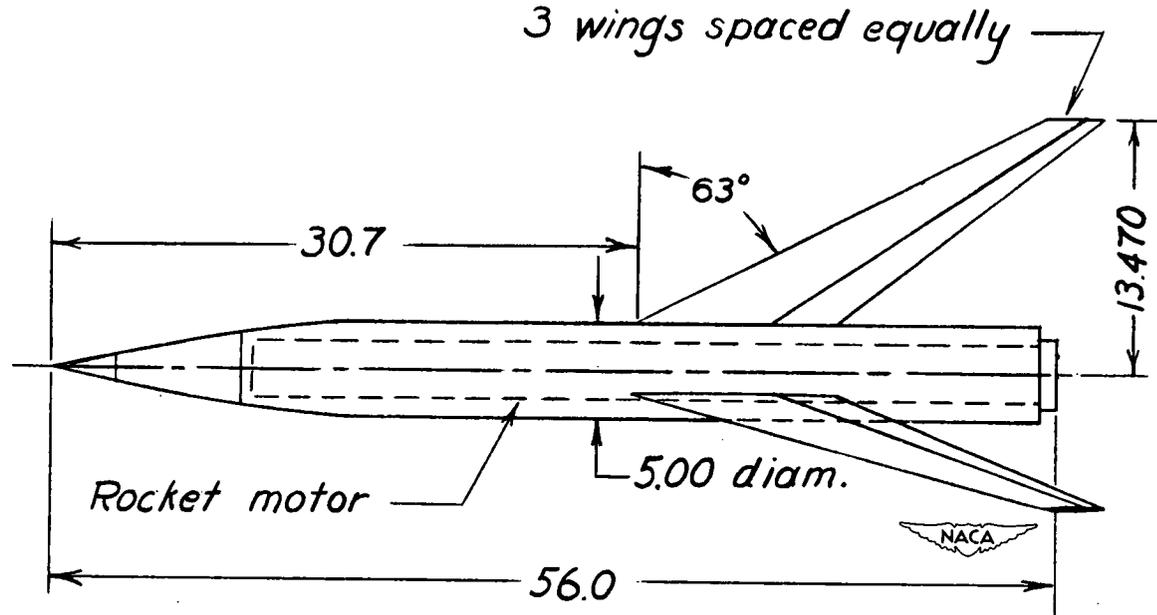
Figure 2.- Sketch of test vehicle showing location of wings $\left(0.814\frac{b}{2} \text{ aileron shown}\right)$. All dimensions are in inches.
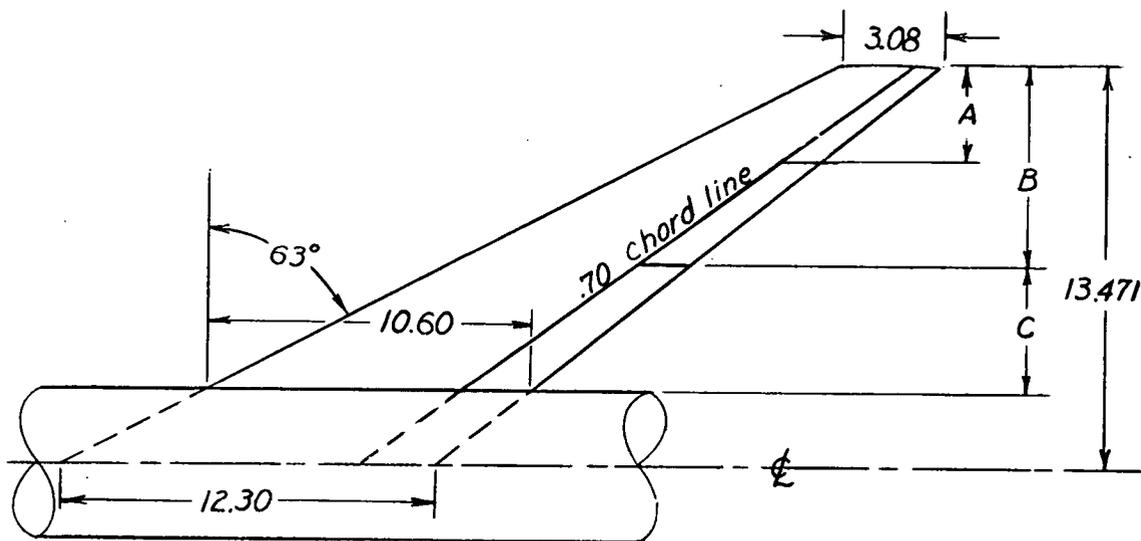
A - 0.25 b/2 outboard aileron · · · · · · · · · · 3.368
B - 0.50 b/2 outboard aileron · · · · · · · · · · 6.735
C - 0.314 b/2 inboard aileron · · · · · · · · · · 4.235
B+C-0.814 b/2 full-span aileron · · · · · · · · · 10.970

(a)   Exposed wing panel.
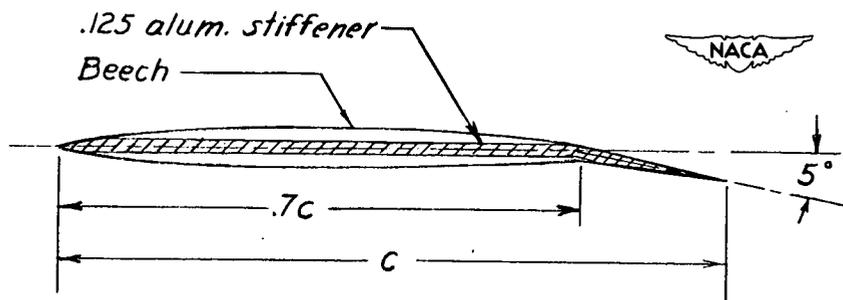
(b)   Composite construction of a typical wing
section parallel to fuselage center line.

Figure 3.- Description of test wings. All dimensions are in inches.
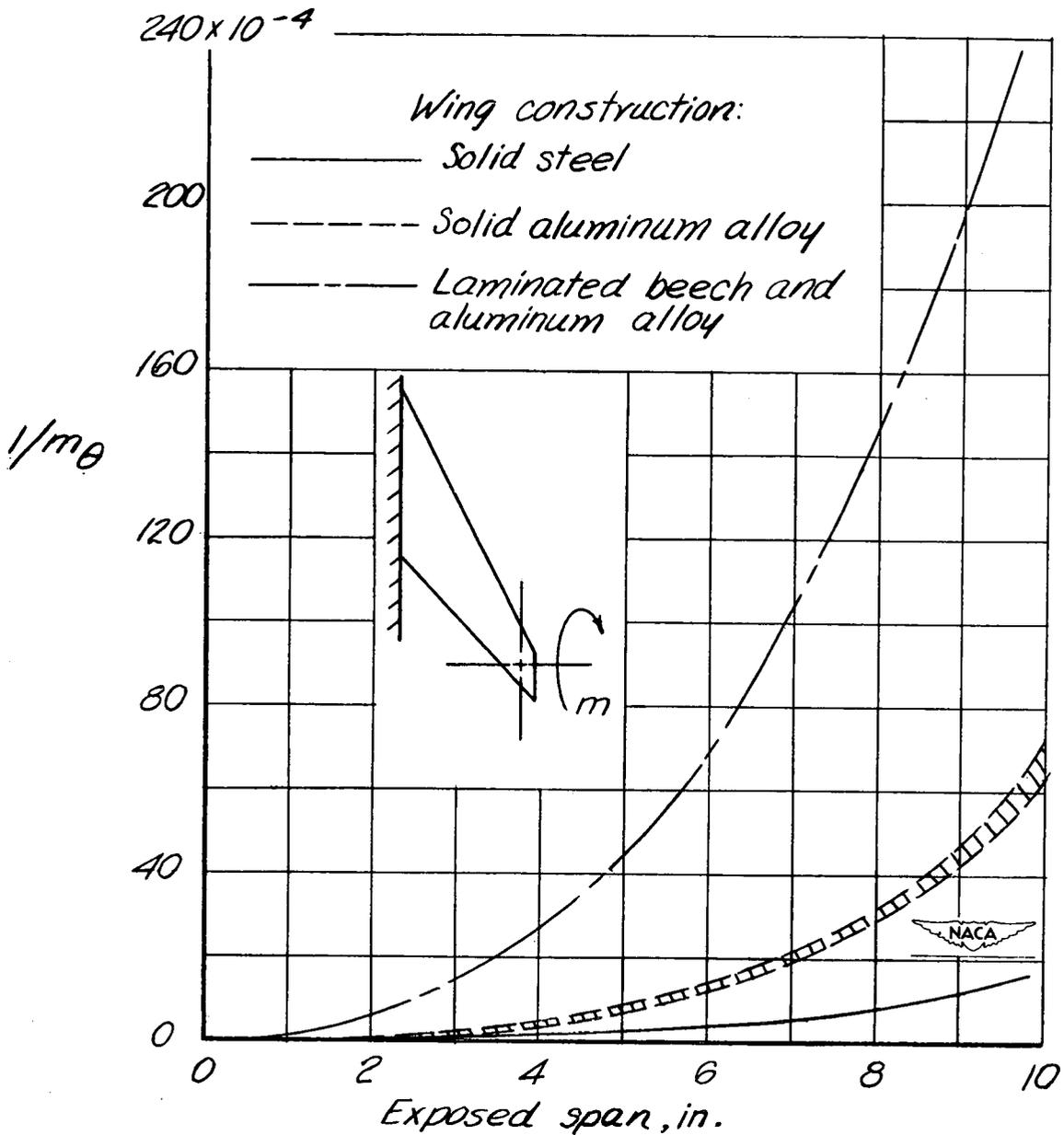
Figure 4.- Variation of wing torsional rigidity with span for several
types of construction.
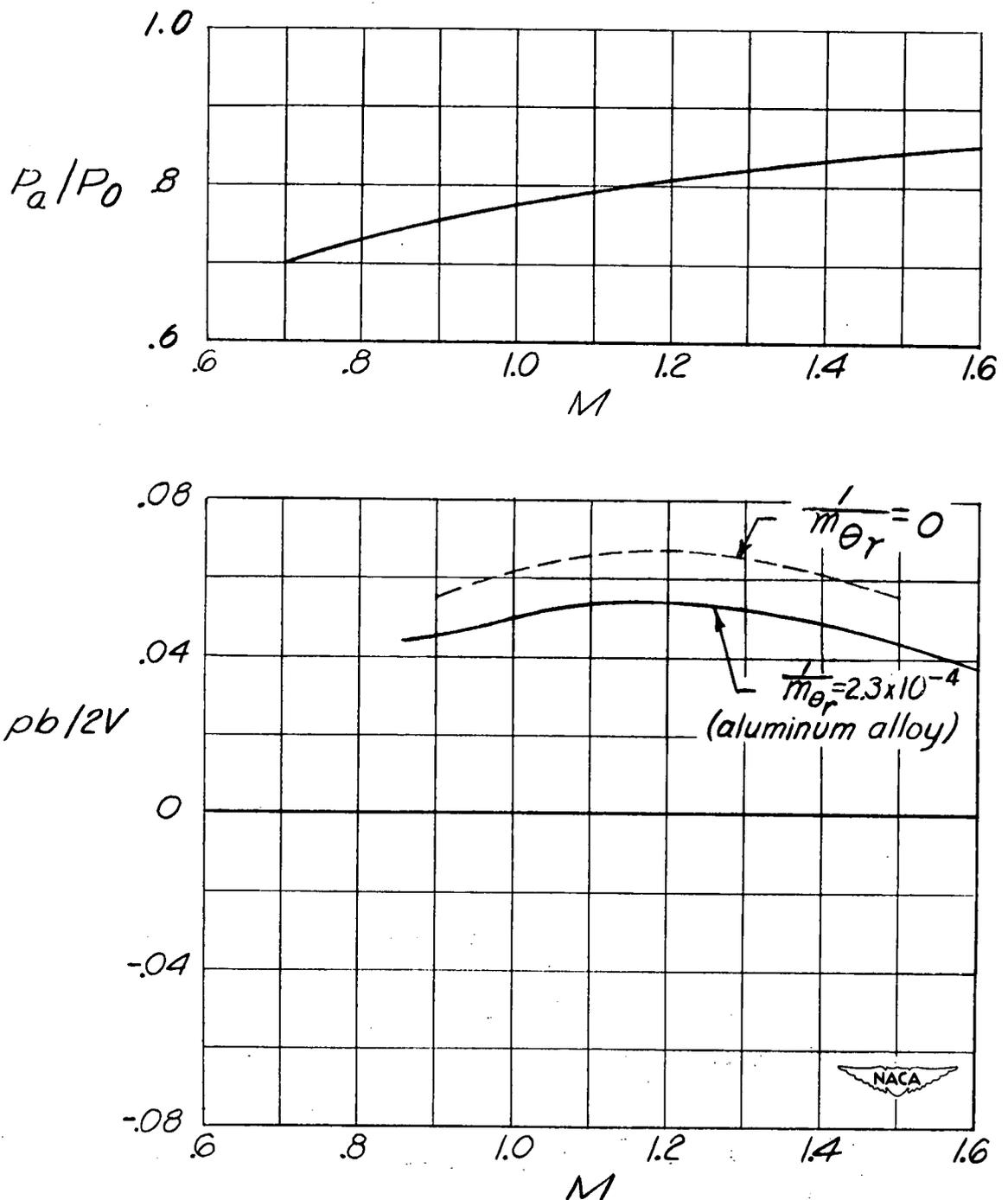
Figure 5.- Variation of pressure ratio and rolling effectiveness with Mach number. Inboard $0.314\frac{b}{2}$ aileron. $\delta_a = 5°$.
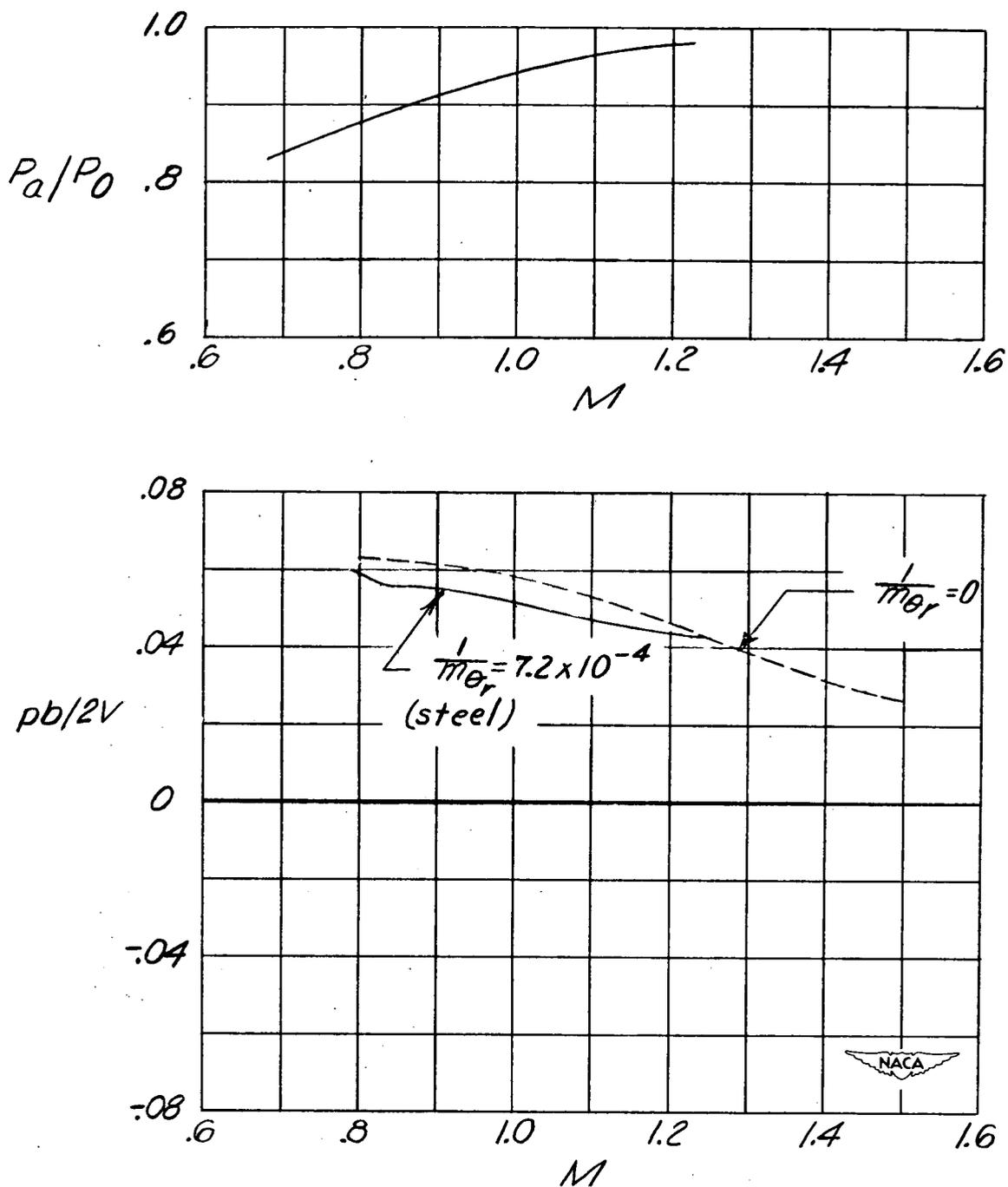
(a) Steel wing.

Figure 6.- Variation of pressure ratio and rolling effectiveness with
Mach number.   Outboard $0.50\frac{b}{2}$ aileron. $\delta_a = 5°$.
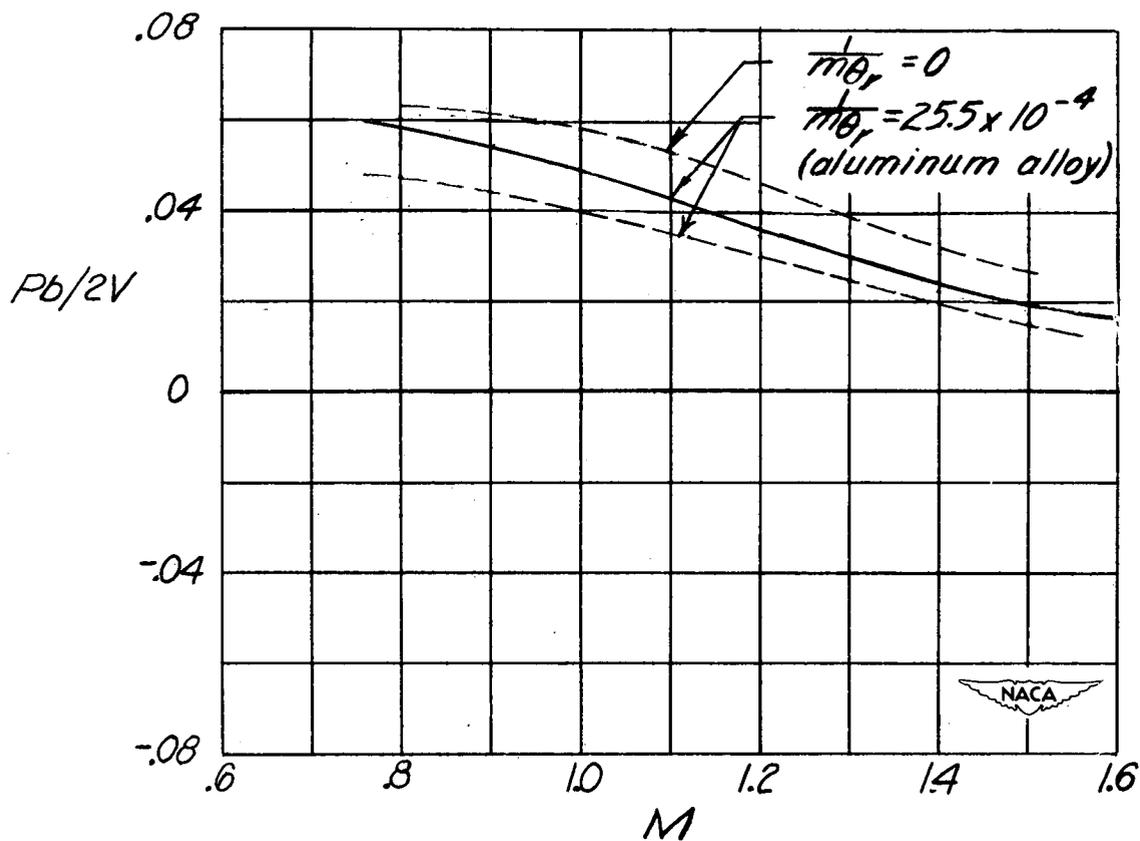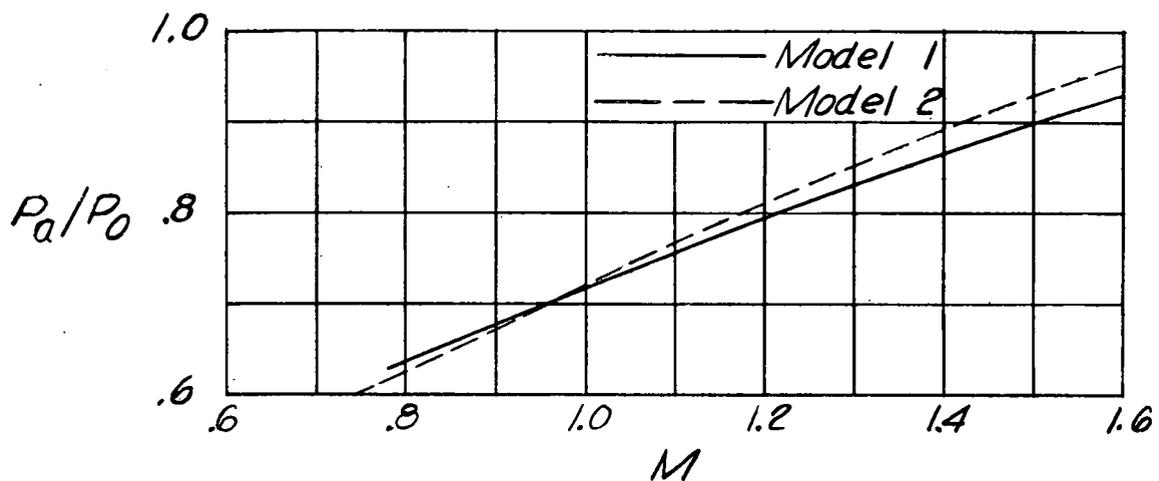
(b)   Aluminum wing.

Figure 6.- Continued.
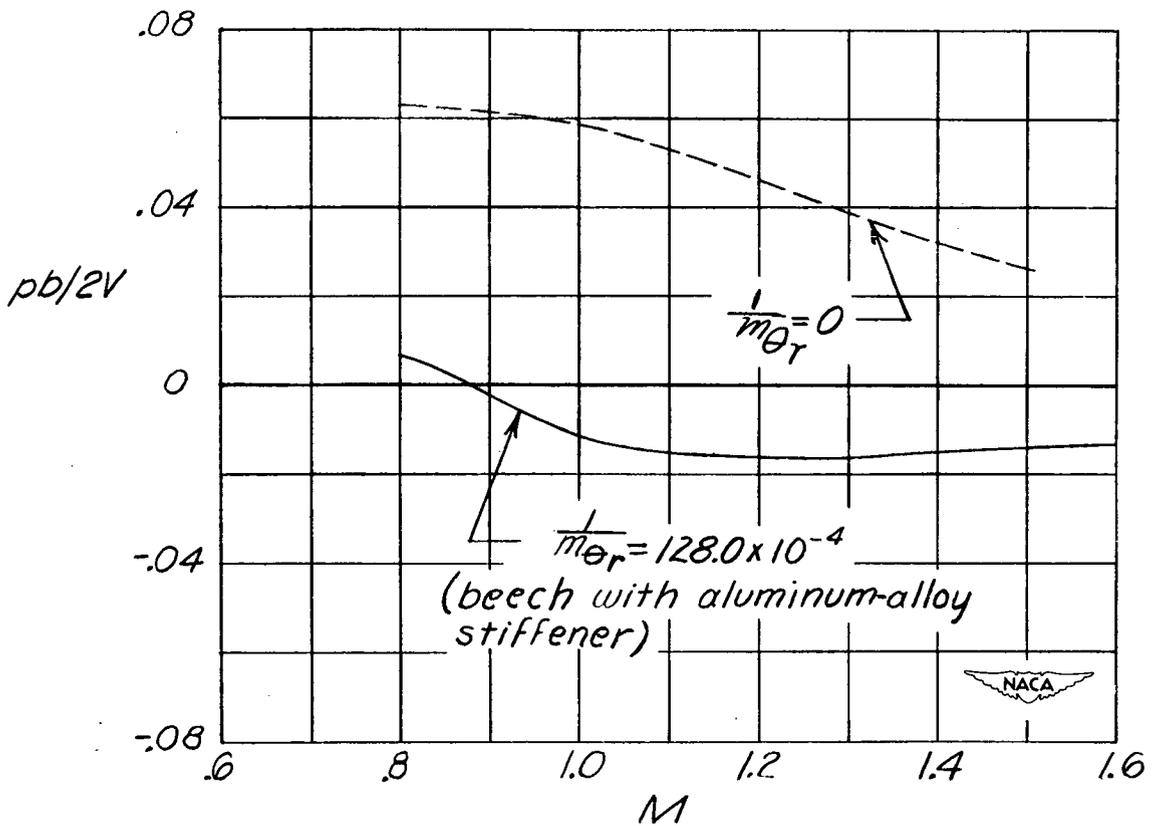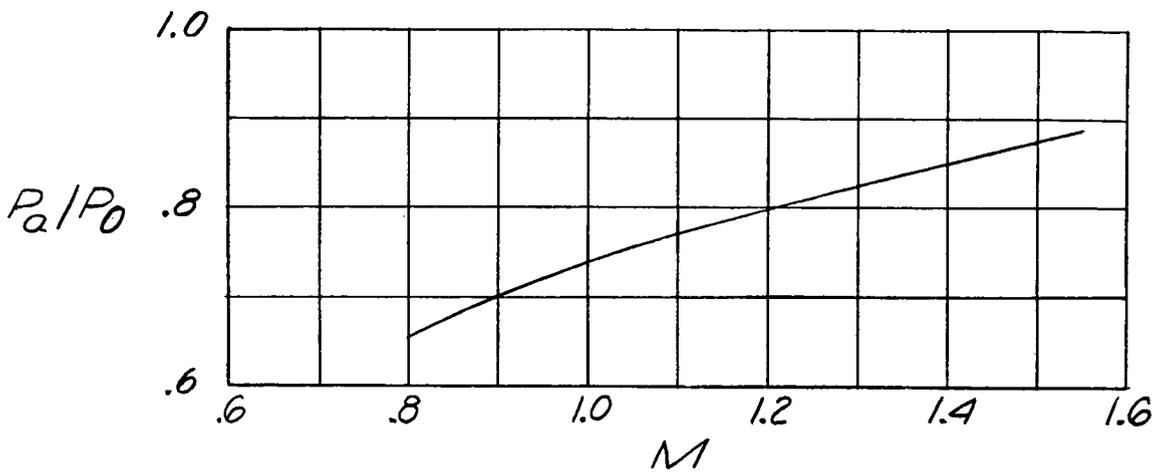
(c) Beech-aluminum wing.

Figure 6.- Concluded.
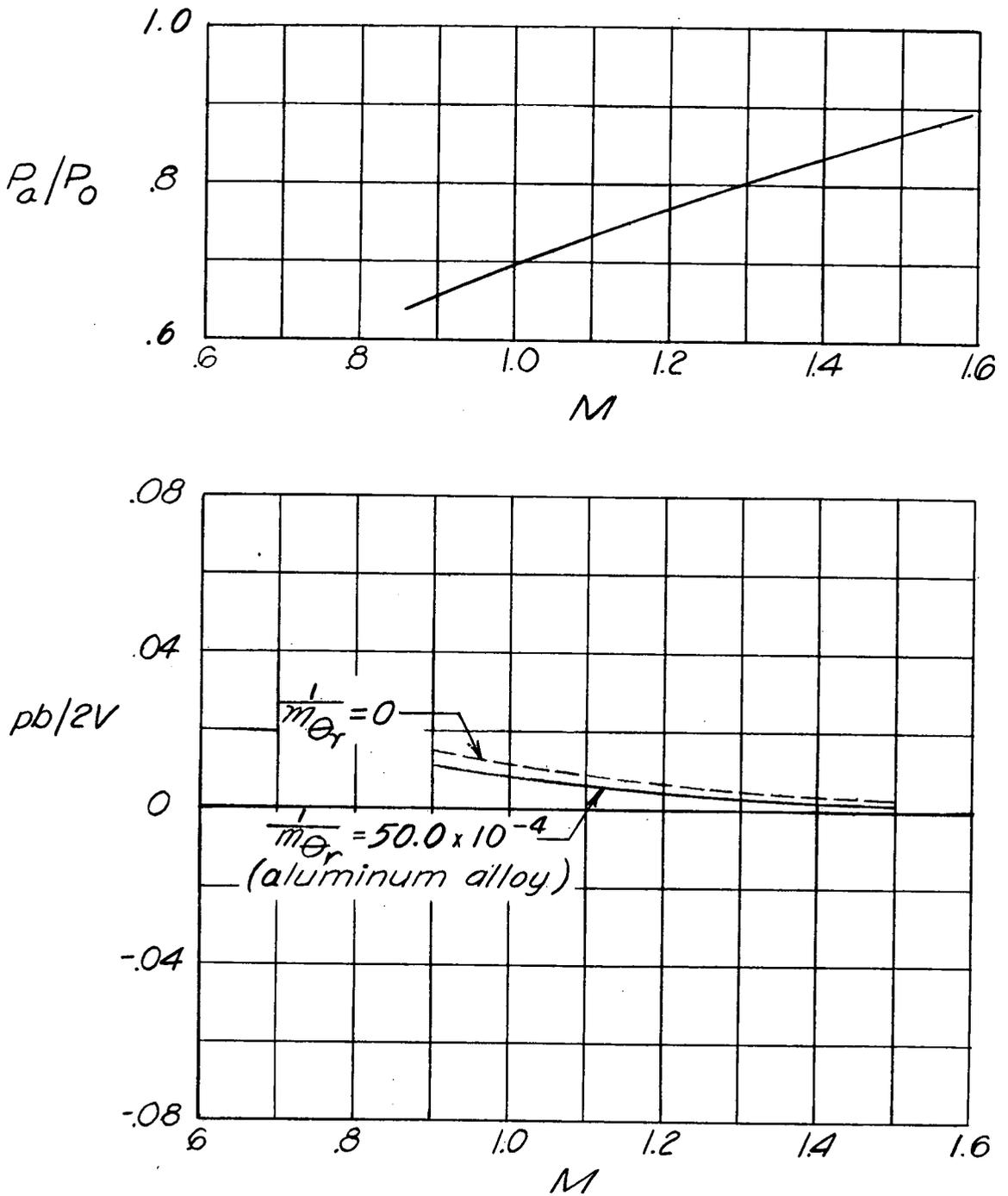
Figure 7.- Variation of pressure ratio and rolling effectiveness with Mach number. Outboard $0.25\frac{b}{2}$ aileron. $\delta_a = 5°$.
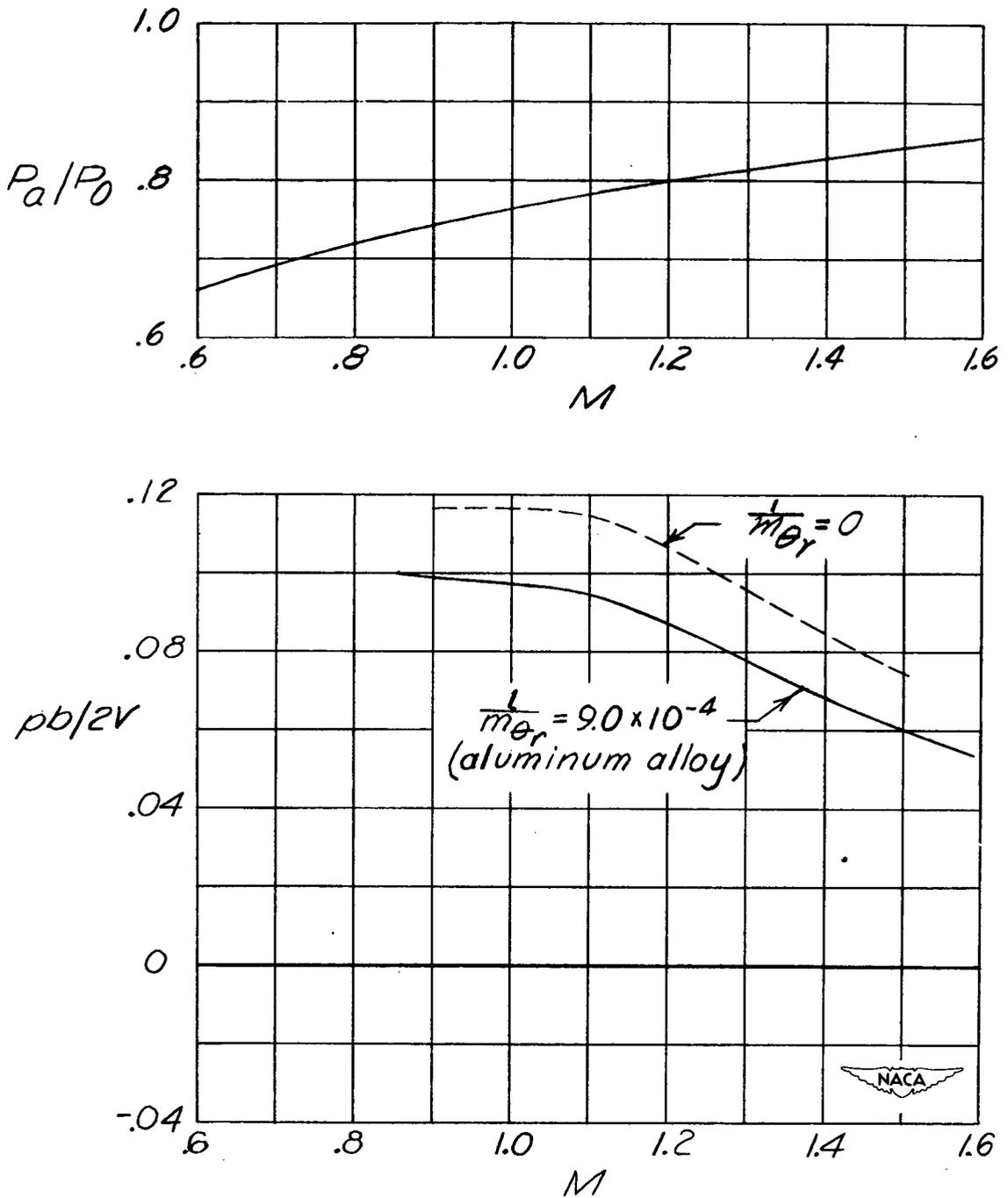
Figure 8.- Variation of pressure ratio and rolling effectiveness with Mach number. $0.814\frac{b}{2}$ aileron. $\delta_a = 5°$.

$$\frac{dc_m/d\delta}{d\alpha/d\delta}$$
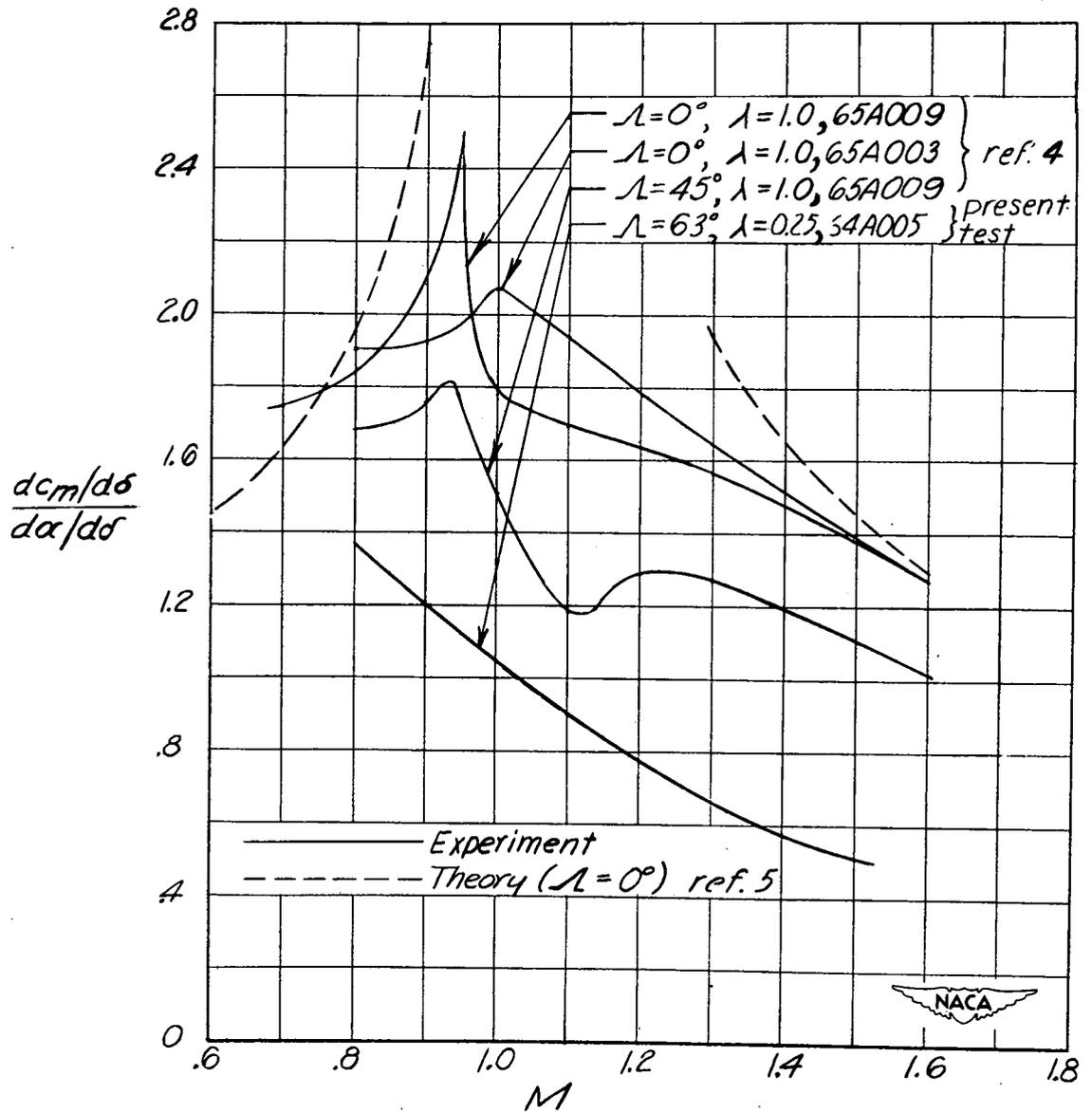
Figure 9.- Variation with Mach number of the effective twisting-moment coefficient evaluated from the experimental rolling-loss data as compared with similar data from reference 4.
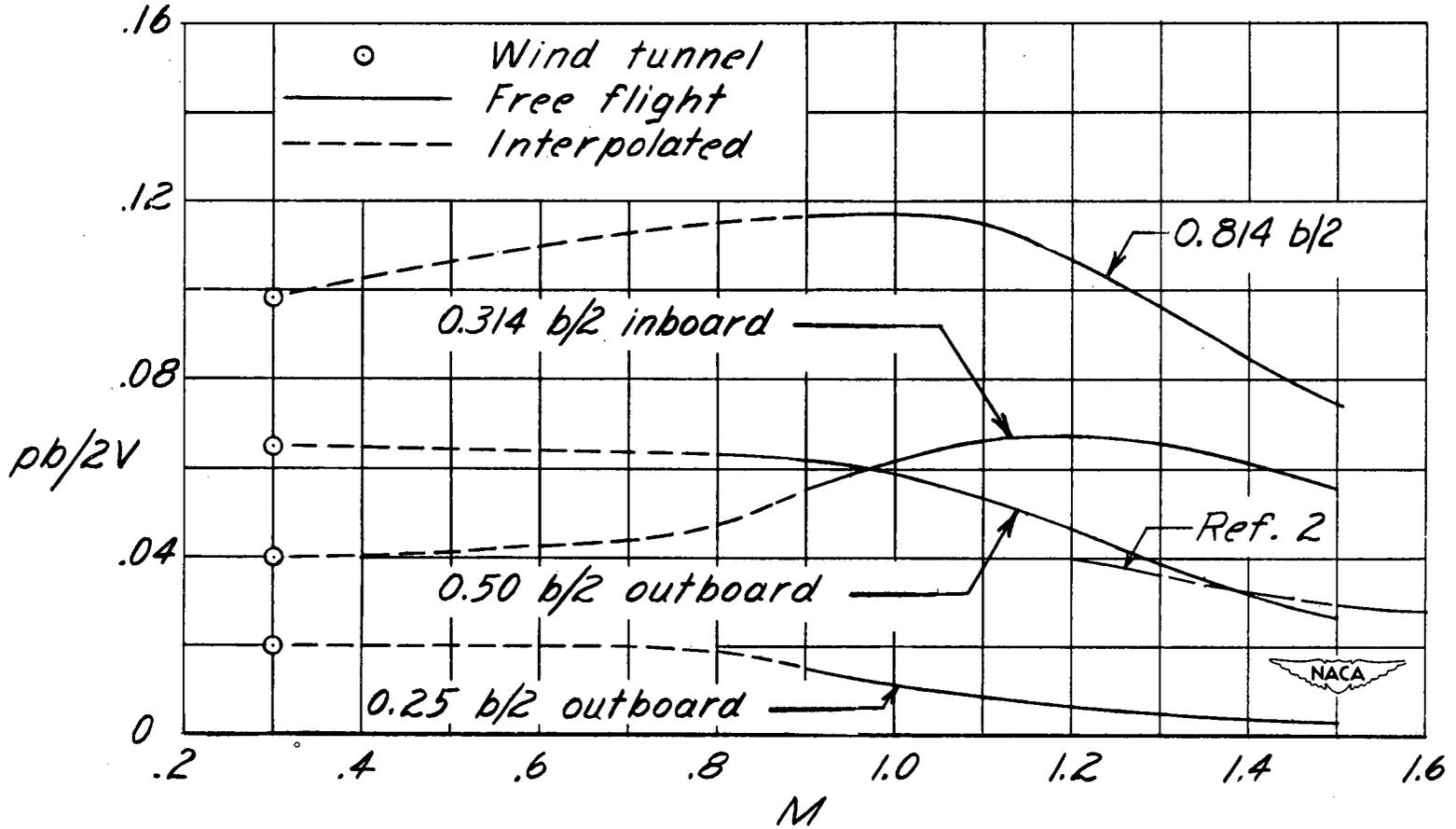
Figure 10.- Effect of spanwise extent of aileron location on the variation of pb/2V with Mach number. $\dfrac{1}{m_{\theta_r}} = 0$; $\delta_a = 5.0^o$.
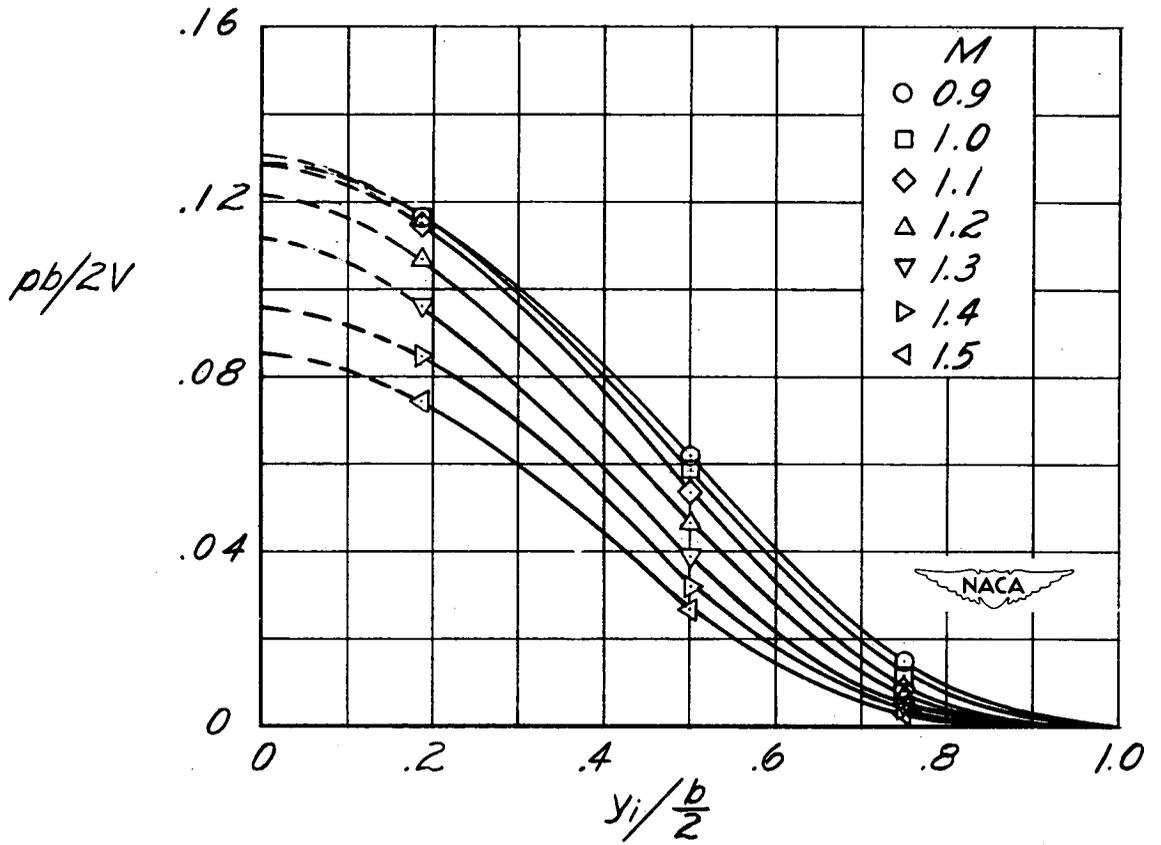
Figure 11.- Variation of rolling effectiveness with aileron span for outboard ailerons. $\frac{1}{m_{\theta_r}} = 0$; $\delta_a = 5^\circ$.
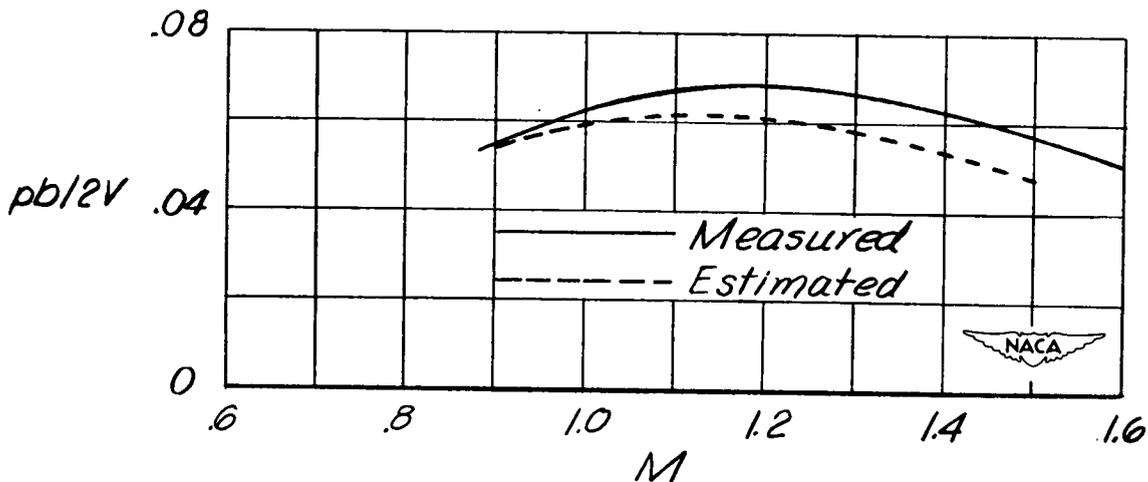
Figure 12.- Comparison of measured rolling effectiveness of inboard $0.314\frac{b}{2}$ aileron with estimated values from figure 11. $\dfrac{1}{m_{\theta_r}} = 0.$